Solvothermal Synthesis, Crystal Structure, and Thermoanalytical Investigations of the New Layered Thioantimonate(III) $[Fe(C_4H_{13}N_3)_2]Sb_6S_{10} \cdot 0.5\ H_2O$

Ralph Stähler,[a] Christian Näther,[a] and Wolfgang Bensch*[a]

Dedicated to Prof. Dr. Hk. Müller-Buschbaum on the occasion of his 70th birthday

Keywords: Thioantimonates / Solvothermal synthesis / Crystal structure / Thermoanalytical measurements

The novel thioantimonate(III) $[Fe(C_4H_{13}N_3)_2]Sb_6S_{10} \cdot 0.5\ H_2O$ was synthesised under mild hydrothermal conditions by allowing elemental Fe, Sb, and S to react in a 50% diethylenetriamine (dien) solution. The compound crystallises in the monoclinic space group $C2/c$ with a = 33.789(3), b = 8.5697(4), c = 24.620(2) Å, β = 118.411(8)°, and V = 6270.3(7) Å^3. In the crystal structure, five SbS_3 trigonal pyramids and one SbS_4 unit are interconnected by sharing common S atoms, forming Sb_2S_2, Sb_4S_4, and Sb_5S_5 heterocycles. The layered $[Sb_6S_{10}]^{2-}$ anion is formed by condensation of the rings in the order Sb_4S_4–Sb_5S_5–Sb_2S_2–Sb_5S_5–Sb_4S_4. The interconnection of the different Sb_xS_x heterocycles leads to the formation of a large $Sb_{16}S_{16}$ ring. The special geometries of the SbS_x units and their interconnection results in a new and unprecedented architecture of the four-atoms thick thioantimonate layer. The calculated bond valence sums (BVS) for the Sb atoms range from 3.07 to 3.16 v. u., indicating that the Sb atoms are formally trivalent. The $[Fe(dien)_2]^{2+}$ cations and the water molecule are located between neighbouring layers. The thermal behaviour of the compound was investigated using DTA-TG measurements. Upon heating decomposition starts at about 200 °C, which is accompanied by the removal of the organic ligands and the incorporated water molecules. In the X-ray powder pattern of the decomposition product, the three compounds Sb_2S_3, $FeSb_2S_4$, and FeS could be identified.

Introduction

In several articles published in the last few years the technologically useful properties of microporous solids have been reviewed in detail.[1−5] The syntheses of such microporous solids are typically carried out under solvothermal conditions in the presence of an organic molecule that should exert a directing effect on the crystallisation process, resulting in the formation of an open-framework inorganic material. The organic species is retained within the cavities or channels of the products. The vast majority of research work is focused on oxidic materials. But chalcogenidometallates with open frameworks have attracted considerable interest because several new compounds are semiconductors and show photoconductivity.[6,7] The syntheses and the structural features of chalcogenidometallates have been recently reviewed.[8,9] A large number of thioantimonates(III) exhibiting different degrees of condensation of the Sb_xS_y anionic fragments were reported.[10−23] In these compounds the linking of the complex anions leads to very different structures. Compounds with one-, two-, and three-dimensional structures were isolated and characterised. Despite the great differences between the thioantimonate(III) structures several structural relationships have been recognised.[9,24] For an insight into the general structural chemistry of the thioantimonates(III) new compounds must be synthesised and characterised. Here we report on the novel compound $[Fe(dien)_2]Sb_6S_{10} \cdot 0.5H_2O$, which adopts a new structure type.

Results and Discussion

The compound $[Fe(dien)_2]Sb_6S_{10} \cdot 0.5\ H_2O$ crystallises in the monoclinic space group $C2/c$ with eight formula units in the unit cell. There are two crystallographically independent Fe^{2+} cations in the asymmetric unit placed in a distorted octahedral environment of two chelating dien ligands (Figure 1: A and B). Hexacoordinated diethylenetriamine complexes of transition group elements have been known for a long time,[25,26] and the geometric isomers of the cations were intensively studied.[25,27−32] The ligand and the cation form fused five-membered rings with conformations that are expected to be different for both isomers. The two independent $[Fe(dien)_2]^{2+}$ cations in $[Fe(dien)_2]Sb_6S_{10} \cdot 0.5\ H_2O$ are meridional [Fe(1)] and *s*-facial [Fe(2)]. We note that $[Fe(dien)_2]^{2+}$ cations have not been reported until now. The Fe−N distances are between 2.185(3) and 2.257(3) Å (Table 1) and comparable with those reported in the literature.[33] The angles N−Fe−N vary between 78.1(2) and 156.2(2)°. As noted before the conformations of the two cations are significantly different and an attempt to fit the two cations onto each other results in a mean root deviation of about 1.5 Å.

Formal valence considerations suggest that all Sb atoms are trivalent. With the exception of Sb(6) each of the crystallographically unique Sb atoms is coordinated by three sulfur atoms with distances Sb−S ranging from 2.3920(8)

[a] Institut für Anorganische Chemie, Universität Kiel, Olshausenstraße 40, 24098 Kiel, Germany

  1434−1948/01/0707−1835 $ 17.50+.50/0

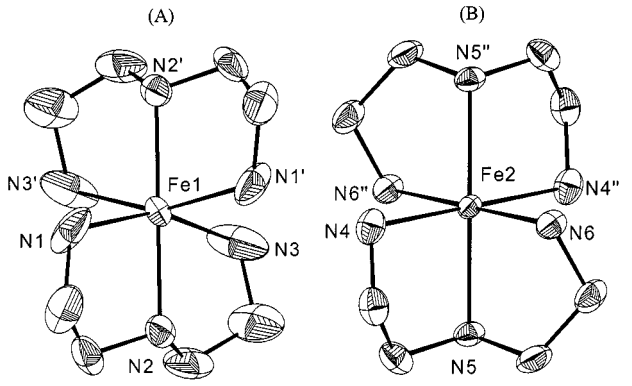

Figure 1. Structures of the two crystallographically independent $[Fe(dien)_2]^{2+}$ cations in the crystal structure of $[Fe(dien)_2]Sb_6S_{10} \cdot 0.5\ H_2O$ with labelling: (A) *mer* isomer and (B) *s-fac* isomer; note: atoms with superscripts are generated by symmetry operations

Table 1. Selected geometric parameters [Å, °] for $[Fe(dien)_2]Sb_6S_{10} \cdot 0.5\ H_2O$

Sb(1)−S(1)	2.4562(7)	Sb(1)−S(4)	2.4331(8)
Sb(1)−S(6)	2.5023(8)	Sb(2)−S(1)	2.4405(8)
Sb(2)−S(2)	2.4560(8)	Sb(2)−S(7)[a]	2.5014(8)
Sb(3)−S(5)	2.3920(8)	Sb(3)−S(3)	2.4691(9)
Sb(3)−S(2)	2.4725(7)	Sb(4)−S(10)[b]	2.4491(8)
Sb(4)−S(4)	2.4594(8)	Sb(4)−S(3)	2.5075(8)
Sb(5)−S(8)	2.3976(8)	Sb(5)−S(6)	2.4283(8)
Sb(5)−S(7)	2.5209(8)	Sb(6)−S(9)	2.4131(8)
Sb(6)−S(10)	2.4824(8)	Sb(6)−S(8)	2.7111(9)
Sb(6)−S(9)[b]	2.7522(8)	Fe(1)−N(1)	2.203(4)
Fe(1)−N(2)	2.185(3)	Fe(1)−N(3)	2.236(4)
Fe(2)−N(4)	2.257(3)	Fe(2)−N(5)	2.228(3)
Fe(2)−N(6)	2.187(3)		
S(4)−Sb(1)−S(1)	98.88(3)	S(4)−Sb(1)−S(6)	86.15(3)
S(1)−Sb(1)−S(6)	81.83(3)	S(1)−Sb(2)−S(2)	99.76(3)
S(1)−Sb(2)−S(7)[a]	88.63(3)	S(2)−Sb(2)−S(7)[a]	87.63(2)
S(5)−Sb(3)−S(3)	98.40(3)	S(5)−Sb(3)−S(2)	96.51(3)
S(3)−Sb(3)−S(2)	95.86(3)	S(10)[b]−Sb(4)−S(4)	92.37(3)
S(10)[b]−Sb(4)−S(3)	85.50(3)	S(4)−Sb(4)−S(3)	94.93(3)
S(8)−Sb(5)−S(6)	101.38(3)	S(8)−Sb(5)−S(7)	91.26(3)
S(6)−Sb(5)−S(7)	92.97(3)	S(9)−Sb(6)−S(10)	95.55(3)
S(9)−Sb(6)−S(8)	89.44(3)	S(10)−Sb(6)−S(8)	88.38(3)
S(9)−Sb(6)−S(9)[b]	88.87(3)	S(10)−Sb(6)−S(9)[b]	90.41(3)
S(8)−Sb(6)−S(9) [b]	177.81(2)	Sb(2)−S(1)−Sb(1)	106.50(3)
Sb(2)−S(2)−Sb(3)	97.65(3)	Sb(3)−S(3)−Sb(4)	97.88(3)
Sb(1)−S(4)−Sb(4)	103.58(3)	Sb(5)−S(6)−Sb(1)	98.79(3)
Sb(2)[a]−S(7)−Sb(5)	99.19(3)	Sb(5)−S(8)−Sb(6)	106.75(3)
Sb(6)−S(9)−Sb(6)[b]	91.13(3)	Sb(4)[b]−S(10)−Sb(6)	101.67(3)

Symmetry codes: [a] $1.5 - x, -0.5 + y, 1.5 - z$. − [b] $1 - x, 2 - y, 1 - z$.

to 2.5209(8) Å (Table 1). The SbS_3 units have an approximately trigonal-pyramidal geometry with angles between 81.83(3) and 106.50(3)° (Table 1). For Sb(6) only two short bonds to S atoms of 2.4131(8) and 2.4824(8) Å are observed, and two longer distances of 2.7111(9) and 2.7522(8) Å (Table 1). The latter distances are longer than expected for single bonds that vary between about 2.4 and 2.6 Å, but they are significantly shorter than the typical so-called secondary bonds with Sb−S distances above around 2.9 Å. Hence, for the further discussion the two S atoms are included in the first coordination sphere of the Sb(6) atom. We note that SbS_4 units with distances between 2.4 and 2.85 Å were reported for $Cs_2Sb_8S_{13}$,[32] $(CH_3NH_3)_2Sb_8S_{13}$,[34] or $Cs_5Sb_8S_{18}(HCO_3)$.[20] All antimony atoms complete their coordination environments with sulfur neighbours at distances between 3.0567(8) and 3.7462(9) (Table 2), which is less than the sum of the van der Waals radii (S_{vdw} + Sb_{vdw} = 3.80 Å).[35] It is noted that the presence of short and long Sb−S distances is often observed in antimony sulfides. The longer Sb−S separations link the primary building blocks yielding higher structural units.

Table 2. Additional long Sb−S bonds [Å]

Sb1−S5	3.1130(9)
Sb1−S7	3.7277(9)
Sb1−S8	3.629(1)
Sb2−S5	3.1651(8)
Sb2−S6[a]	3.5850(8)
Sb2−S6[b]	3.5355(9)
Sb3−S6[b]	3.5048(9)
Sb4−S5	3.3124(9)
Sb4−S9	3.0567(8)
Sb5−S1[c]	3.5424(8)
Sb5−S5[d]	3.3102(8)
Sb6−S4	3.3624(8)
Sb6−S5[d]	3.7462(9)

Symmetry codes: [a] $x, -1 + y, z$. − [b] $1.5 - x, -0.5 + y, 1.5 - z$. − [c] $1.5 - x, 0.5 + y, 1.5 - z$. − [d] $x, 1 + y, z$.

A way to describe the structure of the anion is based on the condensation of different Sb_xS_y heterocycles formed by the interconnection of the SbS_3 and SbS_4 units. The vertex linkage of SbS_3 pyramids involving Sb(1) to Sb(4) leads to

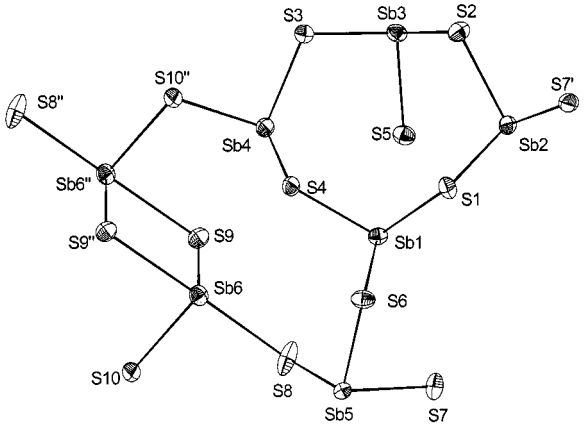

Figure 2. Condensation of the Sb_4S_4 heterocycle and the Sb_3S_8 unit generating an Sb_5S_5 ring; note: atoms denoted with superscripts are generated by symmetry operations

the formation of a puckered Sb_4S_4 ring (Figure 2). A second building-block with composition Sb_3S_8 is composed of two edge-sharing SbS_4 units [Sb(6) and Sb(6a)] being vertex-linked to the Sb(5)S_3 pyramid. The two Sb(6)S_4 units are related by a centre of symmetry forming an Sb_2S_2 ring (Figure 2).

The Sb_3S_8 unit is condensed to the Sb_4S_4 ring via two S atoms [S(6) and S(10a)], resulting in the formation of an

Sb_5S_5 ring [involving Sb(1), Sb(4), Sb(5), Sb(6), and Sb(6a)] (Figure 2). Due to the inversion centre located between the two $Sb(6)S_4$ units, a system of condensed heterocycles with the order $Sb_4S_4-Sb_5S_5-Sb_2S_2-Sb_5S_5-Sb_4S_4$ is generated (Figure 3). The assembly into the final layered anion is achieved by vertex linking of the condensed ring system via the terminal S(7) atoms. Consequently, another large heterocycle with composition $Sb_{16}S_{16}$ is present (shaded area in Figure 3). We note that the layers are four atoms thick, whereas for the overwhelming number of thioantimonates(III) two-atom thick layers are observed.

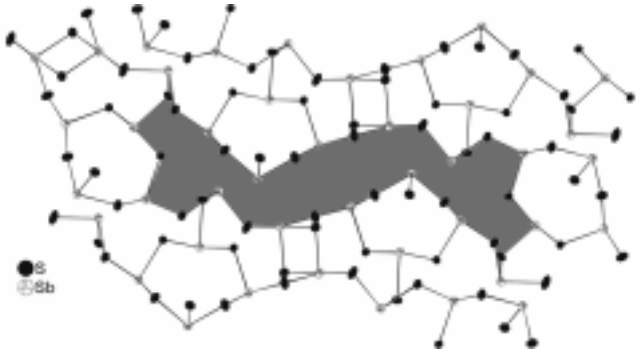

Figure 3. The layered anion with the large $Sb_{16}S_{16}$ ring (shaded area) with displacement ellipsoids drawn at the 50% probability level

The description becomes more complex when the secondary Sb−S bonds are considered. The Sb atoms in the Sb_4S_4 ring have longer Sb−S contacts [Sb(1)−S(5), Sb(1)−S(7), Sb(1)−S(8), Sb(2)−S(5), Sb(2)−S(6A), Sb(2)−S(6B), Sb(3)−S(6B), Sb(4)−S(5), Sb(4)−S(9), Sb(5)−S(1C), Sb(5)−S5(D), Sb(6)−S(4A), Sb(6)−S(5D)] ranging from 3.0567(8) to 3.7462(9) Å (Table 2), enhancing the coordination number from three to six. The atoms Sb(1) and Sb(6) have six neighbours and are in a distorted octahedral environment (Figure 4, B, F). When the s^2 lone pair is treated as a coordination site the polyhedron about Sb(3) may be described as distorted ψ-SbS_4 trigonal-bipyramid. The Sb(4) and Sb(5) atoms have two S neighbours, giving a distorted ψ-SbS_5 octahedron (Figure 4, C, D). With the enhanced coordination environments, different secondary building units can be identified (Figure 4). An Sb_3S_4 semicube (Figure 4, E) involving the two symmetry-related Sb(6) atoms and Sb(4) is formed, which is common in thioantimonates(III).[10,36−39]

The two symmetry-related $Sb(6)S_6$ octahedra share a common edge yielding an Sb_2S_{10} double-octahedron (Figure 4, F). Such a secondary building unit was found in $Cs_2Sb_8S_{13}$[36] and $(CH_3NH_3)_2Sb_8S_{13}$.[37] The three atoms Sb(1), Sb(2), and Sb(4) have secondary bonds to the S(5) atom that is located on top of the crown-like Sb_4S_5 heterocycle (Figure 4, A) thus joining the polyhedra of these Sb atoms of the ring.

The layered anions are within the (−101) plane, and are stacked onto each other parallel to the [110] plane. The cations as well as the water molecule are located between the layers (Figure 5). Six short intermolecular N−H···S distances (Table 3) with H···S distances ranging from 2.460 to 2.959 Å and N−H···S angles between 149.17° and 175.46° are observed, indicative of hydrogen bonding (Table 3).

The crystal structures of many thioantimonates(III) can be described on the basis of the condensation of different Sb_xS_y heterocycles. In the compound $[(CH_3NH_3)_{1.03}K_{2.97}]Sb_{12}S_{20}\cdot 1.34\,H_2O$,[40] in which the anionic part has the same composition when divided by two, the layered $[Sb_{12}S_{20}]^{4-}$ anion is formed by two complex rings having the same composition − $Sb_{12}S_{20}$ − and a very similar shape. Including the S atoms of the different rings (note: in the original contribution only the Sb atoms were counted) an Sb_8S_8 ring and four Sb_3S_3 rings are condensed giving the $Sb_{12}S_{20}$ complex ring system. The complex rings are interconnected into two-atom thick layers by so-called secondary bonds that are between 3.0567(8) and 3.5850(8)

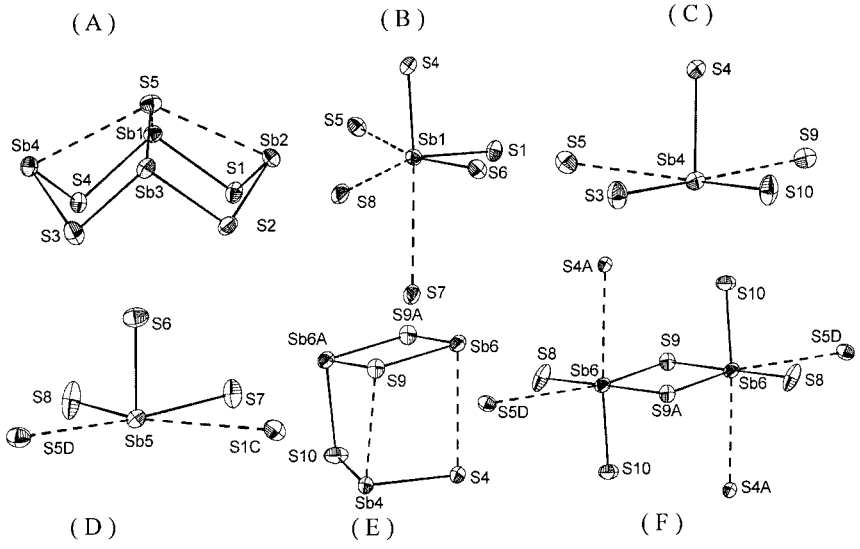

Figure 4. The environments of the Sb atoms with related long secondary bonds (dotted lines); the letters denote symmetry-related atoms (symmetry codes are given in Table 3); the probability ellipsoids are drawn at the 50% level

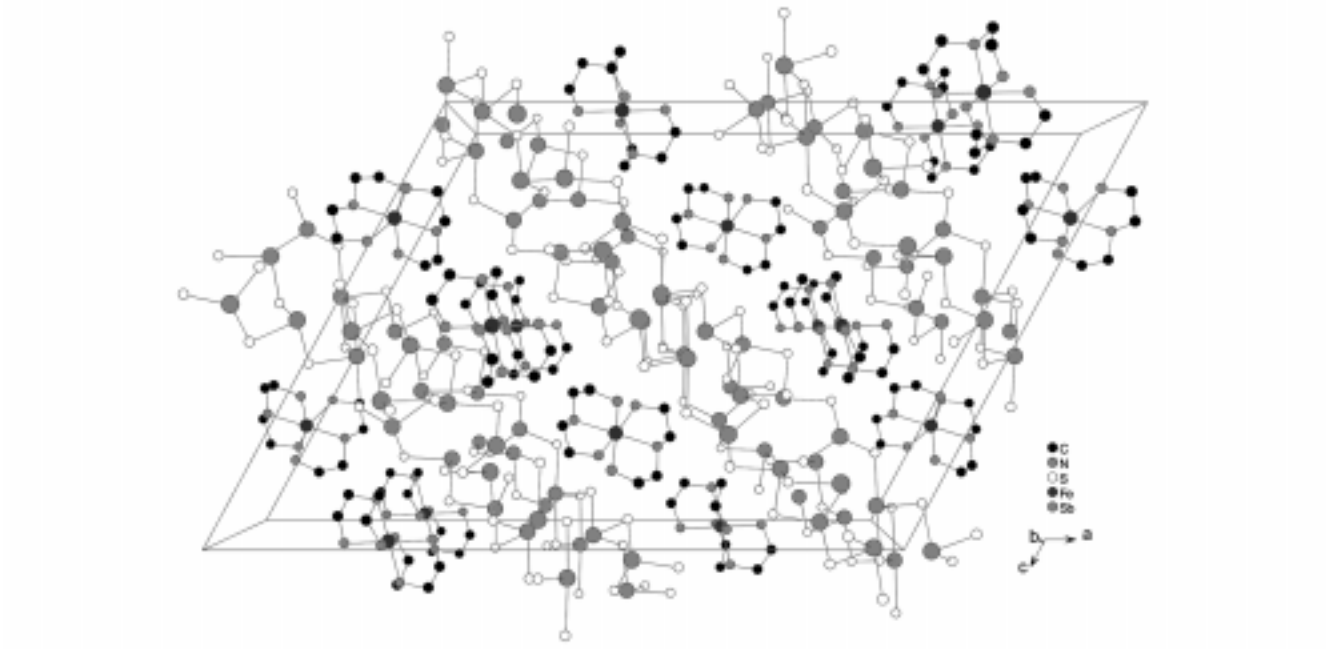

Figure 5. Arrangement of the $[Sb_6S_{10}]^{2-}$ anions and $[Fe(dien)_2]^{2+}$ cations in the crystal structure of $[Fe(C_4H_{13}N_3)_2]Sb_6S_{10} \cdot 0.5\ H_2O$ (water molecules and hydrogen atoms are omitted for clarity)

Table 3. Intermolecular N−H···S contacts and angles [Å, °]

D−H	*d*(H···A)	D−H−A	*A*	D−H	*d*(H···A)	D−H−A	*A*
N4−H6N	2.553	149.54	S2[a]	N2−H3N	2.460	175.46	S8[a]
N6−H10N	2.959	149.17	S2[a]	N1−H2N	2.573	158.67	S9[b]
N3−H5N	2.792	160.47	S3[c]	N1−H1N	2.361	161.21	O1[d]
N5−H8N	2.740	153.55	S7[d]	N3−H4N	2.185	157.36	O1[a]

Symmetry codes: [a] $-x + 3/2, -y + 3/2, -z + 1$. − [b] $-x + 1, y, -z + 3/2$. − [c] $-x + 1, -y + 1, -z + 1$. − [d] $-x + 3/2, y - 1/2, -z + 3/2$.

Å. The compound $[Ph_4P]_2Sb_6S_{10}$[41] contains also an $[Sb_6S_{10}]^{2-}$ anion, but it forms an infinite one-dimensional anionic $(Sb_6S_{10}^{2-})_n$ chain by vertex linkage of SbS_3 pyramids. The interconnection of the pyramids leads to the formation of condensed 10-membered Sb_5S_5 rings with alternating Sb and S atoms. The anionic part of this structure is similar to that reported for $Sb_3S_5{\cdot}N(C_3H_7)_4$.[23] It can be assumed that the size, shape, and charge of the cations determine the dimensionality and the condensation density of the thioantimonate(III) anion.

The Sb_3S_3 rings as well as Sb_4S_4 rings are also found in $[(CH_3CH_2CH_2CH_2NH_2CH_2)_2]_{0.5}Sb_7S_{11}$.[39] In the thioantimonates(III) $[H_3N(CH_2)_3NH_3]Sb_{10}S_{16}$,[42] $(CH_3NH_3)_2Sb_8S_{13}$,[34] $(enH_2)Sb_8S_{13}$ [43], and $(NH_4)_2Sb_4S_7$ [10], the Sb_3S_3 rings are present, and the former two compounds may be viewed as 3-dimensional framework structures when the longer Sb−S contacts are considered.

The bond valence sums (BVS) for the Sb atoms were calculated using the parameters from Brese and O'Keeffe[44] (minimum valence = 0.01). The BVS range from 3.07 to 3.16 v. u. indicating that the Sb atoms formally trivalent. Strong deviations of the calculated BVS from integer numbers are correlated to the stereoactivity of the lone electron pairs (LEP).[45,46] Applying the procedure reported in ref.[47] the BVS of the SbS_x polyhedra are plotted against a parameter $|\Phi|$, which is the length of the vector $\Phi = -\Sigma\Phi_{ij}$ with Φ_{ij} being a vector pointing from Sb_i to the coordinating atom S_j at the distance D_{ij}. The length of Φ_{ij} is given by $\exp(-D_{ij}/0.2)$. The summation is performed over all coordinating S atoms of a polyhedron. For a strong deviation of the spatial distribution of the LEP from spherical symmetry, large $|\Phi|$ values are expected. We observe higher $|\Phi|$ values for Sb(1), Sb(3), and Sb(5), indicating stronger sp^3 character of their LEP.[45] One can assume that the LEP of these Sb^{III} cations are on the opposite side of the three shortest Sb−S bonds of each SbS_3 pyramid.

Thermal Investigations

The thermal behaviour of the title compound was investigated using simultaneous difference thermal analysis and thermogravimetry experiments (Figure 6). Heating selected single crystals of $[Fe(dien)_2]Sb_6S_{10} \cdot 0.5\ H_2O$ under argon a mass loss of 16.5% is observed at T_{onset} = 240.7 °C in the TG curve, which can be attributed to the complete removal

of the dien ligands and the incorporated water molecules $\{-\Delta m_{theor.}[(dien)_2 + 0.5\ H_2O = 16.2\%]\}$. The removal of the ligands is accompanied by two endothermic events at T_P = 261.1 °C and T_P = 277.5 °C. These two peaks were always observed, irrespective of whether large single crystals or powdered samples were used. Such a splitting of the DTA peak during the loss of this organic ligand was also observed for other compounds in which metal cations are surrounded by two dien ligands.[30,47,48] For the present thermal reaction the splitting of the DTA peak is presumably due to a stepwise loss of the ligands, because both cations are in a different environment. In the X-ray powder pattern of the product, the compounds Sb_2S_3, $FeSb_2S_4$, and FeS could be identified. Spectroscopic investigations prove the loss of the organic ligands during the thermal decomposition and elemental analysis shows that only a small amount of carbon and nitrogen is present in the residue (C: 1.11%; N: 0.6%).

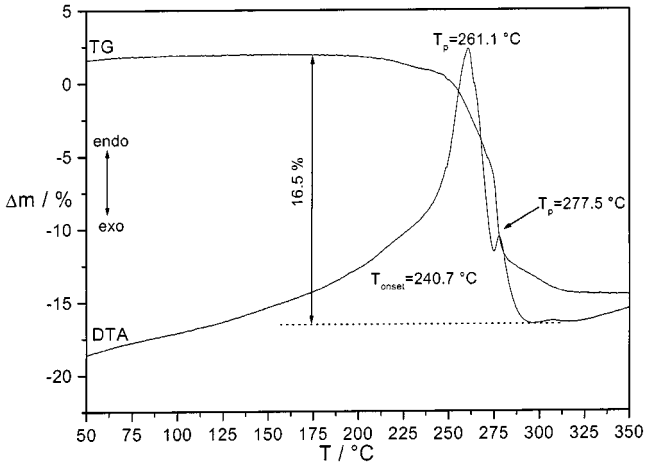

Figure 6. DTA-TG curve for $[Fe(dien)_2]Sb_6S_{10}\cdot 0.5\ H_2O$ (under argon, weight 108.5 mg, powdered crystals, T_p = peak temperature)

Experimental Section

Synthesis: $[Fe(dien)_2]Sb_6S_{10}\cdot 0.5\ H_2O$ (dien = diethylenetriamine) was prepared by treating elemental Fe, Sb, and S in an aqueous solution of dien under solvothermal conditions. In a typical synthesis, 1 mmol of Fe (0.055847 g), 1 mmol of Sb (0.121757 g), and 3 mmol of S (0.032066 g) were added to 10 mL of 50% dien solution. The mixture was heated in a Teflon-lined autoclave at 150 °C for 6 d. The reaction mixture was filtered, washed with water and acetone, and cleaned in an ultrasonic bath. The product consisted of two phases: dark-red needle-like crystals of the title compound as the major phase (yield: 90% based on Sb) and a grey microcrystalline powder as the minor phase, which was amorphous against X-ray powder diffraction. In the by-product the elements iron, sulfur, and antimony were identified with an EDAX analysis.

Structure Determination: Intensities were collected with a STOE Imaging Plate Diffraction System (IPDS) using monochromated Mo-K_α radiation (λ = 0.71073 Å). The intensities were corrected for Lorentz, polarisation, and absorption effects. Structure solution was performed using SHELXS-97.[49] Refinement was done against F^2 using SHELXL-97.[50] All heavy atoms were refined anisotropically. The hydrogen atoms were positioned with idealised geometry and refined with fixed isotropic displacement parameters using a riding model. Technical details of data acquisition and refinement results are summarised in Table 4.

Table 4. Crystallographic data for $[Fe(dien)_2]Sb_6S_{10}\cdot 0.5\ H_2O$

Empirical formula	$[Fe(C_4H_{13}N_3)_2]Sb_6S_{10}\cdot 0.5\ H_2O$
Colour, habit	red needles
Crystal size	0.3 × 0.1 × 0.1 mm
Molecular mass	1321.3 g/mol
Crystal system	monoclinic
Space group	*C*2/*c* (I. T. No. 15)
Calculated density	2.799 g/cm^3
Lattice parameters	
a [Å]	33.789(3) Å
b [Å]]	8.5697(4) Å
c [Å]	24.620(2) Å
β [°]	118.411(8)°
V [Å^3]	6270.3(7) Å^3
Z	8
Temperature	293 K
Scan range	$3.8° \le 2\theta \le 56.3°$
	$-44 \le h \le 44$
	$-9 \le k \le 10$
	$-32 \le l \le 32$
Measured reflections	25723
Independent reflections	7061
Reflections with $F_o > 4\sigma(F_o)$	6304
$R_{int.}$	0.0245
μ	6.22 mm^{-1}
Absorption correction	face-indexed
min./max. trans.	0.3101/0.5057
Extinction correction[a]	$x = 0.00029(2)$
Weight[b]	$y = 0.0377$, $z = 1.2074$
Residual electron density	max. 0.73/min. −0.77 e$^-$/Å^3
*R*1 for all $F_o > 4\sigma(Fo)$	0.0209
*R*1 for all reflections	0.0253
*wR*2 for all $F_o > 4\sigma(F_o)$	0.0508
*wR*2 for all reflections	0.0524
Goodness of fit	1.014

[a] $F^* = F_c\,(k[1 + 0.001 \cdot x \cdot F_c^2 \cdot \lambda^3/\sin(2\theta)]^{-0.25})$. — [b] $w = 1/[\sigma^2(F_o^2) + (y \cdot P)^2 + z \cdot P]$; $P = [\max(F_o^2,0) + 2 \cdot F_c^2]/3$.

Thermoanalytical Measurements: Thermoanalytical measurements were performed using a DTA-TG device STA 429 from Netzsch. All measurements were performed under argon (flow rate 50 mL min^{-1}) with Al_2O_3 crucibles and heating rates of 3 K min^{-1}).

ESEM/EDAX Investigations: Scanning electron microscopic investigations were conducted with the Environmental Scanning Electron Microscope (ESEM XL 30, Fa. Phillips) equipped with an EDAX system.

X-ray Powder Diffractometry: The X-ray powder patterns were recorded with a STOE Stadi-P diffractometer (Co-K_α radiation, λ = 1.788965 Å) in transmission geometry.

Crystallographic data (excluding structure factors) for the structure reported in this paper have been deposited with the Cambridge Crystallographic Data Centre as supplementary publication no. CCDC-151878. Copies of the data can be obtained free of charge on application to CCDC, 12 Union Road, Cambridge CB2 1 EZ, UK [Fax: (internat.) + 44-1223/336-033; E-mail: deposit@ccdc.cam.ac.uk].

Acknowledgments

Many thanks to Prof. Dr. F. Liebau for the calculations of the bond valence values. Financial support by the Deutsche Forschungsgemeinschaft and the State of Schleswig-Holstein is gratefully acknowledged.

[1] M. E. Davis, *Acc. Chem. Res.* **1993**, *26*, 111−115.
[2] M. E. Davis, *Microporous Mesoporous Mater.* **1998**, *21*, 173−182.
[3] G. A. Ozin, A. Kuperman, A. Stein, *Angew. Chem.* **1989**, *101*, 373−390; *Angew. Chem. Int. Ed. Engl.* **1989**, *28*, 59−376.
[4] J. Chen, R. H. Jones, S. Natarajan, J. M. Thomas, *Angew. Chem.* **1994**, *106*, 667−668.
[5] M. T. Weller, S. E. Dann, *Curr. Opinion Solid State Mater. Sci.* **1998**, *3*, 137−143.
[6] U. Simon, F. Schüth, S. Schunk, X. Wang, F. Liebau, *Angew. Chem.* **1997**, *109*, 1138−1142; *Angew. Chem. Int. Ed. Engl.* **1997**, *36*, 1121−1124.
[7] F. Starrost, E. E. Krasovskii, W. Schattke, J. Jockel, U. Simon, X. Wang, F. Liebau, *Phys. Rev. Lett.* **1998**, *80*, 3316−3319.
[8] W. S. Sheldrick, M. Wachhold, *Angew. Chem.* **1997**, *109*, 215−234; *Angew. Chem. Int. Ed. Engl.* **1997**, *36*, 204−224.
[9] W. S. Sheldrick, M. Wachhold, *Coordination Chem. Rev.* **1998**, *176*, 211−322.
[10] G. Dittmar, H. Schäfer, *Z. Anorg. Allg. Chem.* **1977**, *437*, 183−187.
[11] H. A. Graf, H. Schäfer, *Z. Anorg. Allg. Chem.* **1975**, *414*, 220−230.
[12] G. Dittmar, H. Schäfer, *Z. Anorg. Allg. Chem.* **1978**, *441*, 98−102.
[13] B. Eisenmann, H. Schäfer, *Z. Naturforsch., B* **1979**, *34*, 383−385.
[14] G. Cordier, H. Schäfer, C. Schwidetzky, *Z. Naturforsch., B* **1984**, *39*, 131−134.
[15] K. Volk, P. Bickert, R. Kolmer, H. Schäfer, *Z. Naturforsch., B* **1979**, *34*, 380−382.
[16] U. Müller, A. T. Mohammed, *Z. Anorg. Allg. Chem.* **1986**, *533*, 65−72.
[17] B. F. Hoskins, E. R. T. Tiekink, G. Winter, *Inorg. Chim. Acta* **1985**, *99*, 177−186.
[18] M. Schur, W. Bensch, *Z. Anorg. Allg. Chem.* **1998**, *624*, 310−314.
[19] H. Rijnberk, C. Näther, M. Schur, I. Jeß, W. Bensch, *Acta Crystallogr., Sect. C* **1998**, *54*, 920−923.
[20] G. L. Schimek, J. W. Kolis, *Inorg. Chem.* **1997**, *36*, 1689−1693.
[21] K. Volk, H. Schäfer, *Z. Naturforsch., B* **1979**, *34*, 172−175.
[22] J. B. Parise, *Science* **1991**, *251*, 293−294.
[23] J. B. Parise, Y. Ko, *Chem. Mater.* **1992**, *4*, 1446−1450.
[24] K. Tan, Y. Ko, J. B. Parise, J.-H. Park, A. Darovsky, *Chem. Mater.* **1996**, *8*, 493−496.
[25] G. H. Searle, S. F. Lincoln, F. R. Keene, S. G. Teague, D. G. Rowe, *Aust. J. Chem.* **1977**, *30*, 1221−1228.
[26] F. G. Mann, *J. Chem. Soc.* **1934**, 466−474.
[27] F. R. Keene, G. H. Searle, *Inorg. Chem.* **1972**, *11*, 148−156.
[28] Y. Yoshikawa, K. Yamasaki, *Bull. Chem. Soc. Jpn.* **1972**, *45*, 179−184.
[29] G. H. Searle, D. A. House, *Aust. J. Chem.* **1987**, *40*, 361−374.
[30] A. K. Mukherjee, S. Korner, A. Ghosh, N. R. Chaudhuri, M. Mukherjee, A. J. Welch, *J. Chem. Soc., Dalton Trans.* **1994**, 2367−2371.
[31] F. S. Stephens, *J. Chem. Soc.* **1969**, 883−890; F. S. Stephens, *J. Chem. Soc.*, **1969**, 2233−2340.
[32] K. Harada, *Bull. Chem. Soc. Jpn.* **1993**, *66*, 2889−2899.
[33] A. Zalkin, D. H. Templeton, T. Ueki, *Inorg. Chem.* **1973**, *12*, 1641−1646.
[34] X. Wang, F. Liebau, *J. Solid State Chem.* **1994**, *111*, 385−389.
[35] A. Bondi, *J. Phys. Chem.* **1964**, *68*, 441−451.
[36] K. Volk, H. Schäfer, *Z. Naturforsch., B* **1979**, *34*, 1637−1640.
[37] W. Bensch, M. Schur, *Z. Naturforsch., B* **1997**, *52*, 405−409.
[38] H.-O. Stephan, M. G. Kanatzidis, *Inorg. Chem.* **1997**, *36*, 6050−6057.
[39] A. V. Powell, S. Boissiere, A. M. Chippindale, *Chem. Mater.* **2000**, *12*, 182−187.
[40] X. Wang, A. J. Jacobson, F. Liebau, *J. Solid State Chem.* **1998**, *140*, 387−395.
[41] H. Rijnberk, C. Näther, W. Bensch, *Monatsh. Chemie* **2000**, *131*, 721−726.
[42] X. Wang, *Eur. J. Solid State Inorg. Chem.* **1995**, *32*, 303−312.
[43] K. Tan, Y. Ko, J. B. Parise, *Acta Crystallogr., Sect. C* **1994**, *50*, 1439−1442.
[44] N. Brese, M. O'Keeffe, *Acta Crystallogr., Sect. B* **1991**, *47*, 192−197.
[45] X. Wang, F. Liebau, *Acta Crystallogr., Sect. B* **1996**, *52*, 7−15.
[46] X. Wang, F. Liebau, *Z. Kristallogr.* **1996**, *211*, 437−439.
[47] S. Koner, A. Ghosh, N. R. Chaudhuri, *Trans. Met. Chem.* **1988**, *13*, 291−296.
[48] S. Koner, A. Ghosh, N. R. Chaudhuri, *Trans. Met. Chem.* **1990**, *15*, 394−398.
[49] G. M. Sheldrick, *SHELXS-97*, Universität Göttingen, **1997**.
[50] G. M. Sheldrick, *SHELXL-97*, Universität Göttingen, **1997**.

Received November 27, 2000
[I00454]